Batteries & Supercaps

Research Article
doi.org/10.1002/batt.202200306

Chemistry Europe
European Chemical Societies Publishing

www.batteries-supercaps.org

Special Collection

Sustainability and Technical Performance of An All-Organic Aqueous Sodium-Ion Hybrid Supercapacitor

Martin Karlsmo[a] and Patrik Johansson*[a, b]

Development of all-organic aqueous energy storage devices (ESDs) is a promising pathway towards meeting the needs of technically medium/low-demanding electrical applications. Such ESDs should favour low cost, low environmental impact, and safety, and thereby complement more expensive, high voltage, and energy/power dense ESDs such as lithium-ion batteries. Herein, we set out to assemble all-organic aqueous Na-ion hybrid supercapacitors, exclusively using commercial materials, with the aim to provide a *truly* sustainable and low-cost ESD. Overall, the created ESD delivers adequate technical performance in terms of capacity retention, Coulombic efficiency, energy efficiency, and energy/power density. Finally, we apply a straight-forward and qualitative biodegradability method to the ESD.

Introduction

Expensive and sometimes scarce constituents,[1–3] ethically problematic resource origins,[4] and safety concerns,[5,6] all make the lithium-ion battery (LIB) a far from ideal energy storage technology. Still, it is as of today a most necessary technology to enable many high performance demanding electrical applications, that have large overall gains in terms of combatting both pollution and climate change by e.g., promoting electromobility. Not all applications, however, require the performance that LIBs offer in terms of high cell voltages and high energy/power densities. For the former, some applications would in fact benefit from lower cell voltages, e.g., Internet-of-Things (IoT) devices could do without built-in voltage converters if the cell voltage was a mere ca. 1.2–1.5 V.[7,8] With respect to the latter, e.g. large-scale (MWh-TWh) electrochemical energy storage installations, on- or off-grid, with completely different usage patterns, might rather prefer a more affordable price tag and low overall environmental impact, also with respect to the battery production and total energy throughput.[9,10]

In this regard, aqueous electrochemical cells based on organic active materials are especially attractive, as expensive transition metals and flammable organic solvents are both avoided.[11,12] Furthermore, the resource problems of lithium and natural graphite[3] can be tackled by taking advantage of the practically unlimited supply of sodium and by using other types of carbon. Combining all of this we should arguably be able to create very sustainable energy storage devices (ESDs). These ESDs can either be batteries, by combining two redox-active compounds as electrodes, or hybrid supercapacitors (HSCs), by replacing one of them by an electrode attracting charges electrostatically at its surface. The latter can achieve both relatively high energy densities and power densities, as both Faradaic and non-Faradaic processes are employed.[13,14]

Until now, R&D efforts to accomplish such ESDs have, almost without exception, not *really* been all-organic (Table 1). Most often the ESDs had organic electrode active materials, but to be promoted as all-organic and sustainable, a more holistic view is in order, comprising also the binder, separator, current collectors (CCs), and the electrolyte. For example, aqueous water-in-salt electrolytes (WISEs) are almost exclusively based on high concentrations of costly, unsafe, and environmentally unfriendly fluorinated/perchlorate salts;[15–17] the most commonly used PVDF binder is costly, fluorinated and makes use of the likewise costly, toxic and carcinogenic solvent N-methyl-2-pyrrolidone (NMP);[18] and the metal foils applied as substrates and CCs demand mining.[19] All of the above as well as the either glass fibre or polyolefin based (oil-derived) separators needed to complete the cell are laden with large environmental footprints, not the least green-house gas emissions.[20]

Therefore, a *truly* sustainable ESD should rather be assembled from inexpensive and very simple inorganic salts,[21,22] combined with for example cellulose-based binders and separators,[23,24] and carbon-based CCs.[25–27] Furthermore, the active materials should not require complicated synthesis protocols, one of the most critical factors for cost and energy use. While any proper cost analysis using tools such as BatPac[28] to construct cells and packs or by making something like Lazard's Levelized Cost of Storage[29] is very premature, the very design using cheaper materials than is common and reducing the need for dry-rooms should arguably move the cost of the

[a] M. Karlsmo, Prof. P. Johansson
Department of Physics
Chalmers University of Technology
41296 Göteborg, Sweden
E-mail: Patrik.johansson@chalmers.se
[b] Prof. P. Johansson
ALISTORE-ERI, CNRS FR 3104
Hub de l'Energie
80039 Amiens Cedex, France

Supporting information for this article is available on the WWW under https://doi.org/10.1002/batt.202200306

Special Collection *An invited contribution to a Special Collection dedicated to Aqueous Electrolyte Batteries*

Research Article
doi.org/10.1002/batt.202200306

Table 1. Some comparable ESDs – batteries and HSCs – with acronyms used by the referenced papers.

ESD	Cathode	Anode	Binder	Separator	CCs	Aqueous electrolyte	Energy density [Wh kg^{-1}]	Power density [kW kg^{-1}]	Cell voltage	Capacity retention [%]; number of cycles; rate [A g^{-1}]
Hybrid [38]	Carbon microspheres	PNTCDA	PTFE	Glass fibre	SS grid	17 m $NaClO_4$	65	20	2.0	86; 1000; 1.0
Hybrid [25]	ATA polymer	PDI–Ph polymer	PVDF	–ö	Carbon cloth	30 m NH_4Ac	16.5	0.72	1.9	63; 5000; 0.4
Hybrid [39]	Methylene blue@-GO	Polyimide	PTFE	Anion-exchange membrane	Ti mesh	1 M H_2SO_4 and 1 M $(NH_4)_2SO_4$	49	19	1.9	83; 10000; 5.0
Hybrid [*]	AC	PTCDA	CMC	Cellulose paper	Graphite foil	1.9 m Na_2SO_4 + 2.4 m $MgSO_4$	17	4.5	1.5	86; 1000; 1.0
Battery [40]	TCHQ	AQ	PTFE	–	Au mesh	0.5 M H_2SO_4	22	-	1.0	–
Battery [41]	Polytriphenylamine	PNTCDA	PTFE	–	Ti and Ni	21 m LiTFSI	53	32	2.1	85; 700; 0.5
Battery [42]	L–C	P-C	CMC	Celgard 5550	SS	4.4 M K-polyacrylate	16	6.8	1.7	~65; 2500; 0.5
Battery [26]	Polycatechol	Polyimide	PVDF	Glass fibre	Carbon paper	2.5 M $LiNO_3$ + 0.25 M H_2SO_4	81**	348.0**	1.0	80; 1000; 5.0
Battery [43]	Tiron	AQDS	–	Glass fibre	Ti foil	1 M H_2SO_4	29	~0.4	0.9	70; 600; 5 C
Battery [44]	PTMA polymer	NTCDA-EDA polymer	PTFE	–	–	1 M $(NH_4)_2SO_4$	51	15.8	1.9	86; 10000; 5.0
Battery [45]	PTAm	PTPM	–	–	ITO	0.1 M NaCl	–	–	1.7	80; 2000; 60 C
Battery [46]	PLA-PTAm	SBS-PAQE	–	PLA	–	3 M NaCl	–	–	1.6	–
Battery [47]	C/DHB	C/AQ	–	Nafion	AC and Ti	1 M H_2SO_4	10	6.3	1.2	–

* This work. ** Calculated based on the weight of the redox-active unit in the co-polymer.

storage in the right direction. Such an approach would also have the possibility to alter the recycling and circular processes; not only reducing the cost and environmental impact as assembled, but more importantly, at end-of-life (EOL) the ESD could be handled as any organic waste[1][30] e.g., among food left-overs or in the compost to biodegrade.[31]

The latter route, often assisted by bacteria and fungi,[32] has previously been proposed for ESDs, but actually never proven successful.[33–36] Biodegradability has rather been assumed and sometimes claimed based on observing the constituents separately; Lee et al.[34] used a mere $<10\%$ mass loss of their battery components after 120 days to claim biodegradability. Biodegradability is, however, a complex set of phenomena combined, with a variety of definitions, and is hard to quantify, and therefore there exists no single standard. Those that exists are created for industrial and regulatory purposes, such as ISO certifications,[37] with controlled environments and are badly suited for multi-component devices such as ESDs.

Here we build upon our previous work,[21] and further use the excellent rate capability of the perylene-3,4,9,10-tetracarboxylic dianhydride (PTCDA) electrode, as shown in half-cells, to create an all-organic aqueous Na-ion hybrid supercapacitor (Na-HSC) of PTCDA//activated carbon (AC), and subject this to both a variety of characterization techniques as well as performance tests. We do also herein emphasize both active and passive materials to be sustainable and explore this by biodegrading the ESDs created. As passive materials we use sodium carboxymethyl cellulose (CMC) as binder, cellulose paper as separator, graphite foil as CCs, and a combination of sodium/magnesium sulfate salts to create a medium concentrated aqueous electrolyte;[21] all in order to try to limit the scope to achieve a low-cost and environmentally benign ESD, instead of optimizing the electrochemical performance. We start with a proper materials characterization of the electrodes, followed by electrochemical tests of the stand-alone electrodes, and finally we construct full cells and evaluate their functionality as ESDs.

Results and Discussion

First, materials characterization of the electrodes was done using ex situ X-ray diffraction (XRD) and attenuated total reflection Fourier-transform infrared (ATR-FTIR) spectroscopy. Second, the anode (PTCDA) and the cathode (AC) were studied separately in 3-electrode cells to elucidate their individual electrochemical performance, by applying cyclic voltammetry (CV) and galvanostatic cycling (GC) for medium to high scan-rates. Furthermore, electrochemical impedance spectroscopy (EIS) was used to assess the electrolyte and the charge-transfer resistances as associated with the Randles equivalent circuit

[1] Water is not organic, neither are the salts used, but the main point pushed is the implication that these are safer and more sustainable/ecological.

Research Article
doi.org/10.1002/batt.202200306
Chemistry Europe
European Chemical Societies Publishing

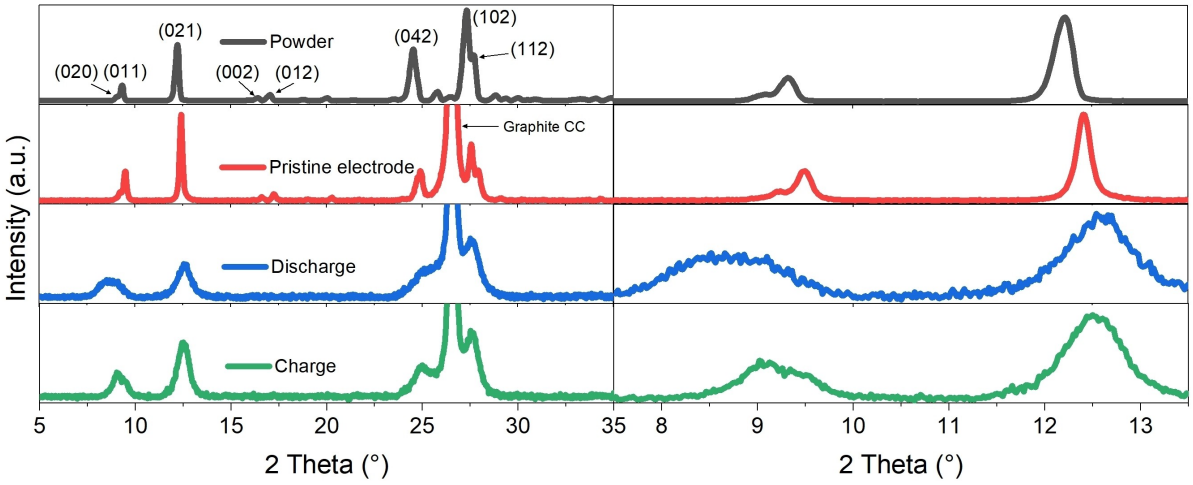

Figure 1. XRD diffractograms (shifted and not in scale w.r.t. intensity) of the PTCDA powder (black), the pristine electrode (red), and electrodes in discharged (blue) and charged (green) states after 20 CV cycles.

model. Thereafter, ESDs of all-organic Na-HSC full cells were assembled and studied electrochemically by GC and EIS, where the resulting energy and power densities as well as the cost and sustainability of the ESD are discussed vs. state-of-the-art. Finally, a biodegradability study was performed and evaluated for the ESDs.

Materials characterization

The XRD on the pure PTCDA powder reveals high crystallinity and data agreeing with the $P2_1/c$ space group with a monoclinic phase.[48] The eight diffraction peaks at *ca.* 9.0°, 9.3°, 12.2°, 16.4°, 17.0°, 24.5°, 27.3°, and 27.7° (Figure 1) correspond to the (020), (011), (021), (002), (012), (042), (102), and (112) planes, respectively, and this clearly confirms the presence of predominantly α-PTCD[2].[49,50] The β-PTCDA diffractogram differs not only by having an additional peak at *ca.* 10° (002), it also does not exhibit the 27.7° (112) peak.[49,51] Moreover, α-PTCDA displays two small peaks, (002) and (012), at 2 Theta $>16°$ whereas β-PTCDA's two small peaks, (020) and (021), are situated at 2 Theta $<16°$.[49] Levin et al. found β-PTCDA (ca. 20%) in PTCDA from Sigma-Aldrich[52] and therefore we suspected that our PTCDA could have had a similar mix, but the diffractogram does not indicate this. The strong peak found at ca. 26.5° for the PTCDA electrodes is attributed to graphite from the CC (Figure S1), resulting from the sample preparation. As compared to pure PTCDA powder, all peaks are slightly upshifted in the electrode diffractogram. This is most likely a result from a shift in the zero due to different sample holders, where the scratched off electrode material was measured at a slightly higher vertical position, and/or a minor alteration in the crystalline PTCDA structure by the binder and conductive additive.

Moreover, the ex situ XRD on the cycled PTCDA electrodes shows that upon sodiation (discharge) the 9.5° peak almost disappears and a new, broader, peak emerges at ca. 8.5°–9° (Figure 1). During the following desodiation (charge), the 8.5° part of the broader peak disappears, the 9.5° peak reappears, suggesting *reversible* structural changes, most likely originating from an expansion due to Na^+ intercalation, similar to Zhou *et al.*'s diffractogram for PTCDA with non-aqueous electrolytes.[53] In contrast, the other part of the broad new peak appearing during sodiation (9°), and remaining during desodiation, indicates an *irreversible* change connected with the electrochemical conditioning process/activation during the first cycles.[54]

The FTIR spectra (Figure S2) have bands at 1594 cm^{-1} and 1774–1732 cm^{-1} that are attributable to the perylene ring and −C=O stretching vibrations, respectively.[49] Both the diffractograms and the spectra of pure PTCDA are similar to those of the pristine electrodes, suggesting no considerable structural changes or side reactions during the electrode preparation process.

Electrochemical characterization

From the CV we first find that after an activation phase during the first cycles, the voltammograms of PTCDA (Figure 2a) display two reversible redox peaks both during oxidation, at ca. −0.4 V and ca. −0.35 V, and during reduction, at ca. −0.7 V and ca. −0.6 V, as in our previous work,[55] and the well-defined shape is maintained for scan rates up to 50 $mV\,s^{-1}$.

From the further analysis of the logarithm of the peak current (i_p) (Figure 2a) using the linear relations [Equation (4)], we find a dominantly battery-type oxidation reaction ($b_{ox} \approx 0.56$) and a pseudo-capacitive reduction reaction ($b_{red} \approx 0.71$).

[2] What we here denote α-PTCDA has previously been named both α-PTCDA and β-PTCDA.

Research Article
doi.org/10.1002/batt.202200306
Chemistry Europe
European Chemical Societies Publishing

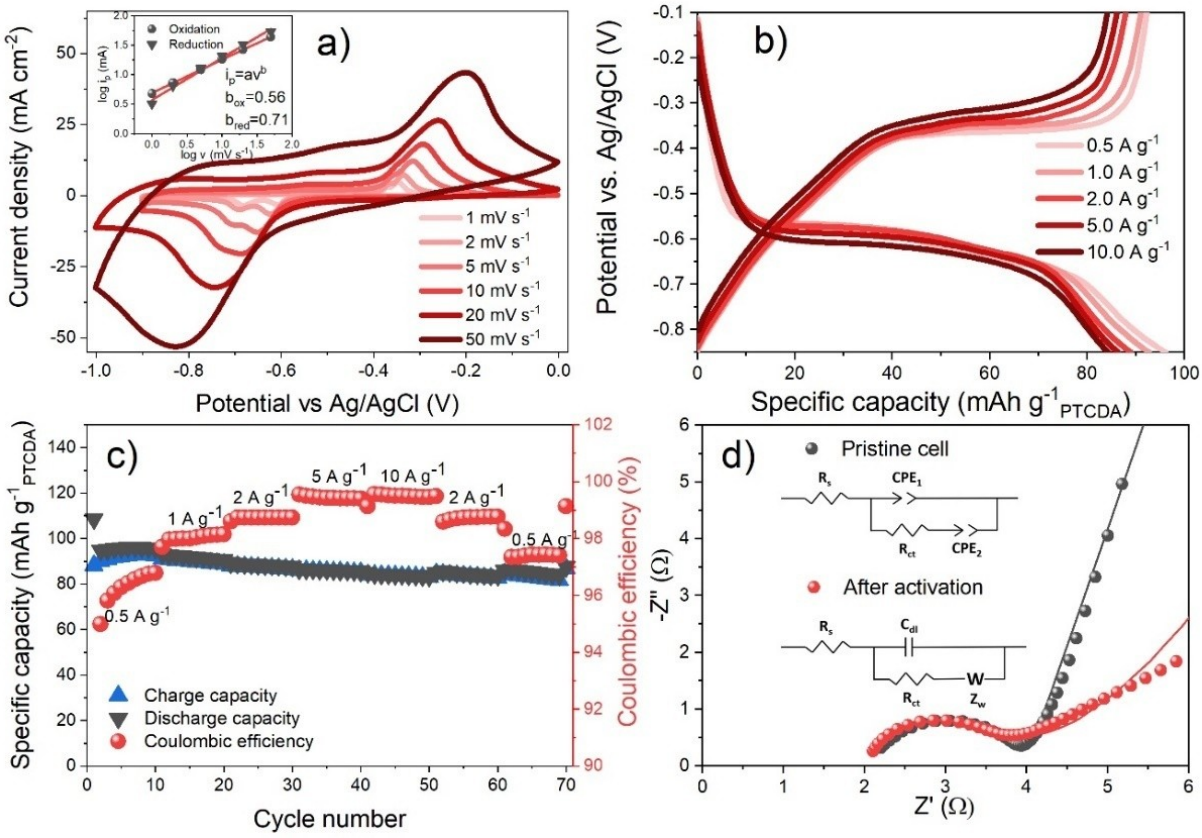

Figure 2. a) Voltammograms, b) galvanostatic charge/discharge curves, c) rate capability test, and d) Nyquist plot for the PTCDA electrodes. Inset in (a) shows log i_p vs. log v.

The extended voltage plateaus of Figure 2(b) are in agreement with the CV data and a two-electron reaction transforming PTCDA to Na_2PTCDA,[54] and maintain their shape as the current density approaches 10 A g^{-1}. At 0.5 A g^{-1} the PTCDA electrode delivers a stable capacity of ca. 92 mAh g^{-1}, which is ca. 30% more than in our previous study[55] and this is attributed to the here lower (ca. 1/3) electrode mass loading. The rate capability test (Figure 2c) shows that the PTCDA electrode can e.g., maintain 91% of the initial capacity at 10 A g^{-1} (~119 C, calculated based on the practical capacity), corresponding to ca. 30 s discharge time, at an excellent Coulombic efficiency. This rate capability exceeds other organic active materials such as PNTCDA with 17 m $NaClO_{4(aq)}$ as electrolyte having ca. 70% rate retention from 5–50 C,[38] P(DA$_{70}$-*stat*-AMPS$_{30}$) and a polyimide with 2.5 M $LiNO_3$ + 0.25 M H_2SO_4, both ca. 85% for 5–60 C ;[26] and PDI–Ph with 30 m NH_4Ac, 83% for 0.5–2 A g^{-1};[25] but significantly better than ATA with 30 m NH_4Ac, only retaining 54% for 0.5–2 A g^{-1}.[25]

From the Nyquist plot, and by implementing the simple and commonly used Randles equivalent circuit cell model, or slightly modified with constant phase elements (CPEs) to appropriately fit the data, the charge-transfer resistance (R_{ct}, 2.0 Ω cm^{-2}) and the electrolyte resistance (R_s, 2.1 Ω cm^{-2}) were extracted at open-circuit voltage (OCV) before cycling (Figure 3d). After the rate test, the resistances were more or less the same, but the angle of the low frequency diffusive region shifts closer to 45°, implying a dominantly diffusion controlled behavior,[56] in agreement with the CV analysis. The R_s and the R_{ct} attained here are akin to the polyimide PNTCDA with 17 m $NaClO_{4(aq)}$ (R_s ca. 2.8 Ω, R_{ct} ca. 8 Ω);[38] whereas PNTCDA (R_s ca. 50 Ω, R_{ct} = 75 Ω) and PTPAn (R_s ca. 40 Ω, R_{ct} = 15 Ω) with 21 m LiTFSI had higher resistances;[41] and Prussian Blue analogues differ quite a lot, ranging from higher (R_s = 7.5 Ω cm^{-2}, R_{ct} = 39 Ω cm^{-2}),[57] to lower resistances (R_s = 0.24 Ω cm^{-2}, R_{ct} = 0.41 Ω cm^{-2}),[58] and to even not having the characteristic semicircle in the Nyquist plot.[59] As we here use 10 mm Ø electrodes, the resistance unit difference is non-significant (1 Ω↔1.27 Ω cm^{-2}). Thus, the PTCDA electrode overall has very agreeable charge transport kinetics and conductivity.

Turning to the AC electrode we, as expected, find log i_p vs. log v slopes close to unity (Figure 3b) and rectangularly shaped voltammograms, characteristic of non-Faradaic processes (Figure 3a), further supported by the charge/discharge curves, as the capacity increases linearly with the applied voltage (Figure 3c). The capacity is ca. 27 mAh g^{-1} at 0.5 A g^{-1}, slightly less than typically achieved,[60,61] but after the initial cycles in the rate capability test, the capacity stabilizes with very good retention throughout (Figure 3d). This activation process has been observed before and is ascribed to the penetration of the electrolyte into the pores of the electrode(s), by the force of the electric field, which prior to cycling were not accessible.[62]

Research Article
doi.org/10.1002/batt.202200306
Chemistry Europe
European Chemical Societies Publishing

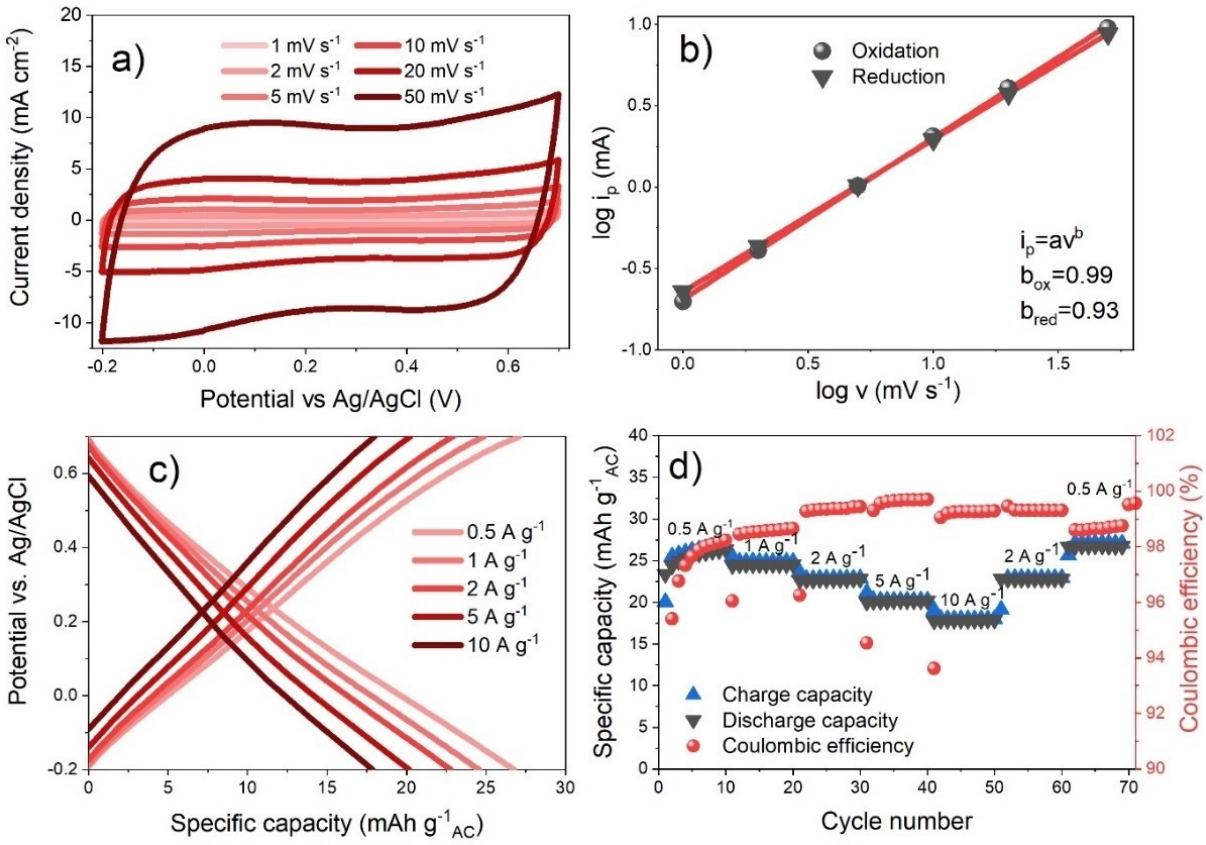

Figure 3. a) Voltammograms, b) log i_p vs. log v, c) galvanostatic charge/discharge curves, and d) rate capability test for the AC electrodes.

The Na-HSC ESD assembled, PTCDA/electrolyte/AC, provides a stable capacity of ca. 22 mAh $g^{-1}_{AC+PTCDA}$ at 0.5 A g^{-1} after the activation process. The rate capability reflects that AC is the rate limiting electrode, at least up to 10 A g^{-1} (Figures 2c, 3d, 4a). The Na-HSC also displays an excellent cycling stability; 86% capacity retention from the 10th to the 1000th cycle at 1.0 A g^{-1}, on par with or exceeding that of the best comparable high-performant "all-organic" aqueous ESDs (Table 1), with a Coulombic efficiency > 98%.

Furthermore, the EIS reveals a drastically decreased R_{ct} (14.6 Ω to 6.6 Ω) (Figure 4d) for the Na-HSC and a $R_{s,\ initial}$ (1.6 Ω cm^{-2}) which stays relatively constant after cycling (Table S1). In comparison, the PDI–Ph//ATA battery mentioned above had resistances ($R_{ct,\ initial}$ = 53 Ω, $R_{s,\ initial}$ = 1.86 Ω) which both slightly increased after cycling.[25] No other EIS analyses of all-organic aqueous ESDs are to be found in the literature.

The energy and power densities of the Na-HSC ESD on the active material level were 17.2 Wh $kg^{-1}_{PTCDA+AC}$ (at 0.5 A g^{-1}) and 4.5 kW $kg^{-1}_{PTCDA+AC}$ (at 50 A g^{-1}), respectively, which by no means surpass the state-of-the-art "all-organic" WISE Na-HSCs (Table 1), but are of the same order of magnitude as many ASIBs and aqueous sodium-ion supercapacitors (SCs) (Figure 4c) with similarly calculated densities. For some perspective, more refined devices such as Skeleton supercapacitor cells offer 5–7 Wh kg^{-1}_{cell} and 20–70 kW kg^{-1}_{cell},[63] while LG Chem E66 A LIBs have 259 Wh kg^{-1}_{cell} and 1.16 kW kg^{-1}_{cell}.[64] The energy efficiency of the Na-HSC was also calculated according to Equation (5) and the resulting 76% is slightly below that of conventional LIB layered oxide cathodes,[65,66] but higher than that of LIB anodes and supercapacitors.[67] It should thus not be a limiting factor for practical implementation.

As a result of the material choices made, the ESD is non-toxic, low-cost (Table S2), and all-organic, and thus could be appropriate for biodegradation at EOL. The ESD had after 4 weeks in the kitchen pre-compost *Bokashi 2.0*, by visual inspection, its original structure intact. This was also the case after 8 weeks dug down in soil (Figure S3). However, the separator had completely degraded and so had parts of the electrode material, while the graphite foil CCs remained unaffected. We therefore approximate the degree of biodegradation by the separator weight decrease: −13%. This is reflected in the literature; cellulose based materials such as Whatman cellulose filter paper and cmC are known to be biodegradable,[68,69] whereas PTCDA is classified as "not rapidly biodegradable" (OECD 301F test) in its safety data sheet. In contrast, AC is used as a biodegradation catalyst,[70] while graphite – one of carbon's most stable allotropes – unsurprisingly did not degrade within 8 weeks.

Thus, to achieve a fully biodegradable ESD, the CCs and AC would most likely need to be replaced. Nevertheless, common items such as paper, orange peel, and wool socks require 2–5 months, 6 months, and 1–5 years to biodegrade,[71] respectively. Therefore, the lack of visible degradation could be due to the

Research Article
doi.org/10.1002/batt.202200306
Chemistry Europe
European Chemical Societies Publishing

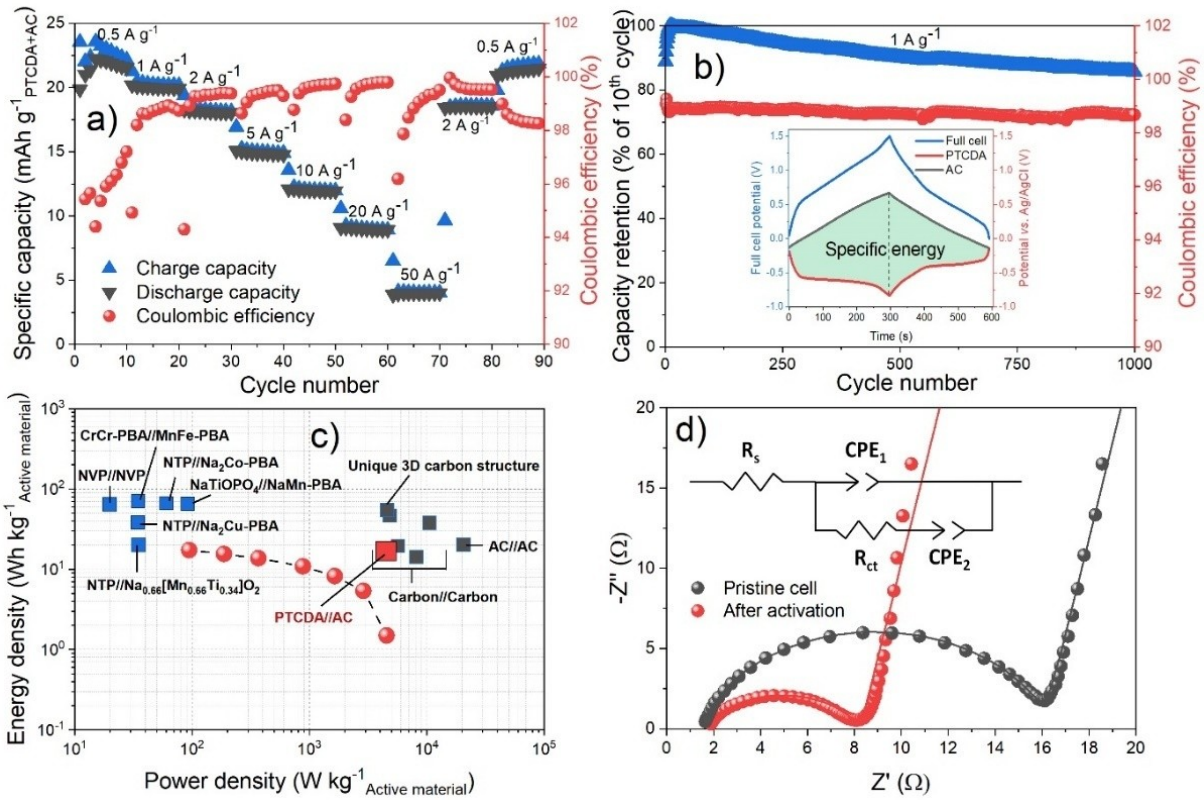

Figure 4. a) Rate capability test, b) GC stability test, c) Ragone plot, and d) Nyquist plot of the Na-HSC with an equivalent circuit. Inset in (b) shows the corresponding charge/discharge curves of the 100th cycle. The Ragone plot contains the most energy dense ASIBs[22,72–76] (blue squares) with arbitrary powder densities (no reported values), the most power dense aqueous Na-ion SCs[77–82] (black squares), with their maximum energy density, and our Na-HSC (red circles and square).

narrow time frame, and our PTCDA-based Na-HSC *could* be biodegradable.

Concluding Remarks

The ESD created reversibly intercalates/deintercalates Na^+ and delivers adequate technical performance in terms of capacity retention, Coulombic efficiency, energy efficiency, and energy/power density. Furthermore, by using not only organic active materials, but also organic binders, separators, and current collectors, and in addition a simple aqueous electrolyte, the created ESD: i) can easily be disposed of as organic waste, ii) is partly biodegradable, and iii) creates a stepping-stone towards safe, low-cost, and low-environmental impact energy storage.

Experimental Section

Electrolyte preparation

Sodium sulfate (Na_2SO_4) (≥99% anhydrous) and magnesium sulfate ($MgSO_4$) (≥99.5% anhydrous), both purchased from Sigma-Aldrich, were used to create a "hybrid electrolyte" (1.9 m Na_2SO_4 + 2.4 m $MgSO_4$), as introduced in our previous study.[55] This was done by first dissolving Na_2SO_4 to saturation in ultra-pure water (Millipore® Direct-Q® Purification, 18.2 MΩ cm at 25 °C), before adding $MgSO_4$, all made in magnet stirred vials.

Electrode fabrication

The PTCDA (Sigma-Aldrich) based electrodes employed herein were similar to those used in Ref. [55] but had a lower loading. They were made by first preparing a solution of 3 wt% cmC (Sigma-Aldrich) in ultra-pure water until complete dissolution by stirring. Subsequently, PTCDA and carbon black (CB) (Ketjenblack EC-300 J) were mixed manually with a mortar before being added to the cmC solution and stirred for 12 h. The slurry was casted onto A graphite foil (SGL Carbon) using a Doctor blade (400 μm wet thickness) followed by vacuum drying at 60 °C for 12 h. The electrode weight ratio PTCDA:CB:CMC was 75:15:10 with a final thickness of ~40 μm and a loading of 0.7–1.0 mg cm^{-2} active material. AC (Darco G-60, 600 m^2 g^{-1}, J.T. Baker) was first stirred for 12 h in an aqueous 1 M HNO_3 solution, then washed with excessive amounts of ultra-pure water, followed by vacuum drying at 100 °C for 12 h. The same procedure and weight ratio as for PTCDA was used to create the AC electrodes used in the ESDs, but with a 500 μm wet thickness which resulted in a final thickness of ~100 μm and an active material loading of 2.0-3.5 mg cm^{-2}.

The free-standing AC electrodes, used in the electrochemical characterization of the stand-alone electrodes, but not in the EDSs, were made by mixing AC, CB (Acetylene Black, 100% compressed, Alfa Aesar), and PTFE (60 wt% in solution, Sigma-Aldrich) in a 75:15:10 weight ratio, following the procedure described by Brousse et al.[83] After adding acetone, the solution was stirred and

heated at 55 °C until the solvent had evaporated. The resulting paste was kneaded and spread with ca. 1 mL ethanol until resulting in a homogeneous film. The free-standing electrode was dried at 60 °C in an oven for 12 h, with a resulting thickness of ~400 μm and a loading of 10–12 mg cm^{-2} active material.

Materials characterization

PTCDA electrodes were pre-cycled 20 times to charged and discharged states by CV between −0.15 and −0.9 V vs. Ag/AgCl at 1.0 mV s^{-1} using a Biologic VMP3 multichannel potentiostat/galvanostat. Post cycling, the electrodes were recovered and washed with 1–2 mL ultra-pure water. After drying in ambient air, ex situ XRD was performed on electrode material that had been scratched off from the CC, using a single crystal sample holder and a Bruker D8 Discover equipment to obtain diffractograms in the range 5°–35° 2 Theta. In the preparation stage some CC material was unavoidably scratched off as well. The pure PTCDA powder was measured using a standard sample holder levelled with the surface. Cu radiation was used with a Ni filter to cut Cu K_β contributions, with two 2.5° soller slits to improve peak shapes. The incidence slit was set to Fixed Sample Illumination mode with 5 mm illumination, and an anti-scatter shield was placed 2 mm above the samples. The samples were measured with 0.02° increments, and 1 s per step, summing up to 1500 s per scan, while rotated at 10 rpm.

FTIR vibrational spectra were obtained using a Bruker Alpha ATR-FTIR spectrometer and A ge crystal. For each sample 512 scans with a resolution of 2 cm^{-1} were made.

Electrochemical and battery assessments

The GC, CV, and EIS studies were carried out using a Biologic VMP3 multichannel potentiostat/galvanostat. 3-electrode Swagelok cells were assembled with a PTCDA working electrode (WE) and a free-standing AC counter electrode (CE), both 10 mm Ø, and an Ag/AgCl reference electrode (RE) (5 mm Ø, 0.127 mm silver foil, Alfa Aesar/AgCl ink, ALS Japan) together with a Whatman cellulose filter separator (Grade 44, Sigma-Aldrich). The AC electrode characterization was done in a symmetric AC electrode (10 mm Ø) cell with a CE/WE weight ratio of at least 2. Scan rates of 1–50 mV s^{-1} and potential ranges between 0 and −0.9/−1.0 V (PTCDA) or −0.2 and 0.7 V (AC) vs. Ag/AgCl were used for the CV. Rate capability tests were performed between −0.1 and −0.8 V (PTCDA) or −0.2 and 0.7 V (AC) *vs.* Ag/AgCl at current densities from 0.5 A g^{-1} to 10 A g^{-1}. EIS was carried out on 3-electrode cells from 100 kHz to 100 mHz with a sinusoidal perturbation of 5 mV, prior to and after the above-described rate capability tests at OCV.

Na-HSCs full cells were put together from PTCDA CEs and AC WEs in 3-electrode Swagelok cells to be able to monitor fall electrode potentials, with PTCDA:AC weight ratios of *ca.* 1:3 to balance the capacity. Current densities from 0.5 A g^{-1} to 50 A g^{-1} were applied from 0 to 1.55 V. GC was performed at 1.0 A g^{-1} from 0 to 1.5 V for 1000 cycles. EIS was done in the same manner as described above, but for the 2-electrode coin cells (CR2032) 25 μL of electrolyte was used, whereas 50 μL was used for *all* other cells.

The EIS spectra were fitted using *ZView 4* with equivalent circuit models similar to the Randles equivalent circuit model.

The active material level specific capacitance C_{sp} (F g^{-1}) of the Na-HSCs was calculated as:

$$C_{sp} = \frac{I}{m\left(\frac{dV}{dt}\right)}, \quad (1)$$

from the galvanostatic charge-discharge profiles, where I (mA) is the discharge current and m (mg) is the total mass of active material in both electrodes.

The cell level specific energy density E (Wh kg^{-1}) and *ditto* power density P (W·kg^{-1}) were then calculated as:

$$E = \frac{C_{sp} \cdot \Delta V^2}{7.6}, \quad (2)$$

$$P = \frac{E}{\Delta t} \cdot 3600, \quad (3)$$

where $\triangle V$ (V) is the discharge voltage range and $\triangle t$ (s) is the discharge time.

The logarithm of the peak current (i_p) was plotted *vs.* the sweep rate (v), and the b parameter from:

$$\log i_p = b \cdot \log v + \log a, \quad (4)$$

and used to determine if the current originates from Faradaic redox reactions or non-Faradaic capacitive behaviour. The former generates $b \approx 0.5$, and the latter $b \approx 1.0$.[84]

Finally, the energy efficiency was calculated as the ratio between the specific energy of discharge *vs.* charge ($E_{discharge}/E_{charge}$), as extracted from areas between curves for the 100th cycle in the GC stability test.

Biodegradability study

A PTCDA//AC Na-HSC of *ca.* 5 x 5 cm with punched out (10 mm Ø) holes[3] was clamped together with a Whatman cellulose filter separator and 1 mL of hybrid electrolyte. The Na-HSC was put into a *Bokashi 2.0* kitchen compost for 4 weeks together with 1–2 kg restaurant food left-overs and *Bokashiströ* (wheat bran with lactic acid bacteria, yeasts, and photosynthetic bacteria). After this pre-composting, the Na-HSC was dug down in a plant pot (50 cm Ø) of commercial gardening soil (40–60 l) for 8 weeks.

Acknowledgements

We would like to express our sincere appreciation to the Swedish Research Council for Sustainable Development (FORMAS) for supporting this work. We also thank Prof. Lars Öhrström (Dept. of Chemistry, Chalmers) and Dr. Michal Strach (Chalmers Materials Analysis Laboratory) for their help and expertise with the XRD measurements and analysis.

Conflict of Interest

The authors declare no conflict of interest.

[3] Left-over material after punching out electrodes to the Swagelok cells.

Data Availability Statement

The data that support the findings of this study are available from the corresponding author upon reasonable request.

Keywords: all-organic · aqueous electrolyte · battery-supercapacitor hybrid · hybrid ion capacitor · sodium-ion capacitor · supercapattery

[1] G. Martin, L. Rentsch, M. Höck, M. Bertau, *Energy Storage Mater.* **2017**, *6*, 171–179.
[2] V. A. Oltean, S. Renault, M. Valvo, D. Brandell, *Materials (Basel).* **2016**, *9*, DOI 10.3390/ma9030142.
[3] G. A. Blengini, C. E. L. Latunussa, U. Eynard, C. Torres de Matos, D. Wittmer, K. Georgitzikis, C. Pavel, S. Carrara, L. Mancini, M. Unguru, D. Blagoeva, F. Mathieux, D. Pennington, *Study on the EU's List of Critical Raw Materials (2020) Final Report*, Publications Office Of The European Union, **2020**.
[4] "Democratic Republic of Congo: 'This is what we die for': Human rights abuses in the Democratic Republic of the Congo power the global trade in cobalt | Amnesty International," can be found under https://www.amnesty.org/en/documents/afr62/3183/2016/en/, **n.d.**
[5] L. J. Vimmerstedt, S. Ring, C. J. Hammel, *Current Status of Environmental, Health, and Safety Issues of Lithium Ion Electric Vehicle Batteries*, Golden, CO, **1995**.
[6] A. Hammami, N. Raymond, M. Armand, *Nature* **2003**, *424*, 635–636.
[7] A. Richelli, M. Salem, L. Colalongo, *Energies* **2021**, *14*, 5419.
[8] A. Richelli, L. Colalongo, S. Tonoli, Z. M. Kovács-Vajna, *IEEE Trans. Power Electron.* **2009**, *24*, 1541–1546.
[9] H. S. Hirsh, Y. Li, D. H. S. Tan, M. Zhang, E. Zhao, Y. Shirley Meng, *Adv. Energy Mater.* **2020**, *10*, 2001274.
[10] A. Ponrouch, D. Monti, A. Boschin, B. Steen, P. Johansson, M. R. Palacín, *J. Mater. Chem. A* **2014**, *3*, 22–42.
[11] Y. Chen, Y. Kang, Y. Zhao, L. Wang, J. Liu, Y. Li, Z. Liang, X. He, X. Li, N. Tavajohi, B. Li, *J. Energy Chem.* **2021**, *59*, 83–99.
[12] Z. Song, H. Zhou, *Energy Environ. Sci.* **2013**, *6*, 2280–2301.
[13] B. Zhao, D. Chen, X. Xiong, B. Song, R. Hu, Q. Zhang, B. H. Rainwater, G. H. Waller, D. Zhen, Y. Ding, Y. Chen, C. Qu, D. Dang, C. P. Wong, M. Liu, *Energy Storage Mater.* **2017**, *7*, 32–39.
[14] S. Wu, Y. Chen, T. Jiao, J. Zhou, J. Cheng, B. Liu, S. Yang, K. Zhang, W. Zhang, S. Wu, Y. Chen, J. Zhou, S. Yang, K. Zhang, T. Jiao, J. Cheng, B. Liu, W. Zhang, *Adv. Energy Mater.* **2019**, *9*, 1902915.
[15] L. Suo, O. Borodin, T. Gao, M. Olguin, J. Ho, X. Fan, C. Luo, C. Wang, K. Xu, *Science* **2015**, *350*, 938–943.
[16] R. S. Kühnel, D. Reber, C. Battaglia, *ACS Energy Lett.* **2017**, *2*, 2005–2006.
[17] J. Yin, C. Zheng, L. Qi, H. Wang, *J. Power Sources* **2011**, *196*, 4080–4087.
[18] D. Bresser, D. Buchholz, A. Moretti, A. Varzi, S. Passerini, *Energy Environ. Sci.* **2018**, *11*, 3096–3127.
[19] S. H. Farjana, N. Huda, M. A. Parvez Mahmud, R. Saidur, *J. Cleaner Prod.* **2019**, *231*, 1200–1217.
[20] S. V. Joshi, L. T. Drzal, A. K. Mohanty, S. Arora, *Composites Part A* **2004**, *35*, 371–376.
[21] M. Karlsmo, R. Bouchal, P. Johansson, *Angew. Chem. Int. Ed.* **2021**, *60*, 24709–24715.
[22] X. Y. Wu, M. Y. Sun, Y. F. Shen, J. F. Qian, Y. L. Cao, X. P. Ai, H. X. Yang, *ChemSusChem* **2014**, *7*, 407–411.
[23] T. C. Nirmale, B. B. Kale, A. J. Varma, *Int. J. Biol. Macromol.* **2017**, *103*, 1032–1043.
[24] J. Sheng, S. Tong, Z. He, R. Yang, *Cellul.* **2017**, *24*, 4103–4122.
[25] K. C. S. Lakshmi, X. Ji, T.-Y. Chen, B. Vedhanarayanan, T.-W. Lin, *J. Power Sources* **2021**, *511*, 230434.
[26] N. Patil, A. Mavrandonakis, C. Jérôme, C. Detrembleur, N. Casado, D. Mecerreyes, J. Palma, R. Marcilla, *J. Mater. Chem. A* **2021**, *9*, 505–514.
[27] Z. Zhou, N. Li, Y. Yang, H. Chen, S. Jiao, W.-L. Song, D. Fang, Z. Zhou, N. Li, Y. Yang, H. Chen, W. Song, D. Fang, S. Jiao, *Adv. Energy Mater.* **2018**, *8*, 1801439.
[28] "BatPaC: Battery Manufacturing Cost Estimation | Argonne National Laboratory," can be found under https://www.anl.gov/partnerships/batpac-battery-manufacturing-cost-estimation, **n.d.**
[29] "Lazard.com | Levelized Cost Of Energy, Levelized Cost Of Storage, and Levelized Cost Of Hydrogen," can be found under https://www.lazard.com/perspective/levelized-cost-of-energy-levelized-cost-of-storage-and-levelized-cost-of-hydrogen/, **n.d.**
[30] A. Khalid, M. Arshad, M. Anjum, T. Mahmood, L. Dawson, *Waste Manage.* **2011**, *31*, 1737–1744.
[31] M. Alexander, *Biodegradation and Bioremediation*, Gulf Professional Publishing, **1999**.
[32] D. D. Focht, *Access Sci.* **2020**, DOI 10.1036/1097-8542.422025.
[33] C. Chen, Y. Zhang, Y. Li, J. Dai, J. Song, Y. Yao, Y. Gong, I. Kierzewski, J. Xie, L. Hu, *Energy Environ. Sci.* **2017**, *10*, 538–545.
[34] M. H. Lee, J. Lee, S.-K. Jung, D. Kang, M. S. Park, G. D. Cha, K. W. Cho, J.-H. Song, S. Moon, Y. S. Yun, S. J. Kim, Y. W. Lim, D.-H. Kim, K. Kang, *Adv. Mater.* **2021**, *33*, 2004902.
[35] G. Colherinhas, T. Malaspina, E. E. Fileti, *ACS Omega* **2018**, *3*, 13869–13875.
[36] M.-J. Park, J.-S. Lee, *Adv. Electron. Mater.* **2019**, *5*, 1800411.
[37] A. Krzan, S. Hemjinda, S. Miertus, A. Corti, E. Chiellini, *Polym. Degrad. Stab.* **2006**, *91*, 2819–2833.
[38] Y. Zhang, P. Nie, C. Xu, G. Xu, B. Ding, H. Dou, X. Zhang, *Electrochim. Acta* **2018**, *268*, 512–519.
[39] Y. Zhang, Y. An, L. Wu, H. Chen, Z. Li, H. Dou, V. Murugadoss, J. Fan, X. Zhang, X. Mai, Z. Guo, *J. Mater. Chem. A* **2019**, *7*, 19668–19675.
[40] T. Tomai, S. Mitani, D. Komatsu, Y. Kawaguchi, I. Honma, *Sci. Reports 2014 41* **2014**, *4*, 1–6.
[41] X. Dong, H. Yu, Y. Ma, J. L. Bao, D. G. Truhlar, Y. Wang, Y. Xia, *Chem. A Eur. J.* **2017**, *23*, 2560–2565.
[42] Z. Khan, U. Ail, F. N. Ajjan, J. Phopase, Z. U. Khan, N. Kim, J. Nilsson, O. Inganäs, M. Berggren, X. Crispin, *Adv. Energy Sustain. Res.* **2022**, *3*, 2100165.
[43] Y. Xu, Y. Zheng, C. Wang, Q. Chen, *ACS Appl. Mater. Interfaces* **2019**, *11*, 23222–23228.
[44] Y. Zhang, Y. An, B. Yin, J. Jiang, S. Dong, H. Dou, X. Zhang, *J. Mater. Chem. A* **2019**, *7*, 11314–11320.
[45] N. Sano, W. Tomita, S. Hara, C.-M. Min, J.-S. Lee, K. Oyaizu, H. Nishide, *ACS Appl. Mater. Interfaces* **2013**, *5*, 1355–1361.
[46] K. Hatakeyama-Sato, H. Wakamatsu, K. Yamagishi, T. Fujie, S. Takeoka, K. Oyaizu, H. Nishide, *Small* **2019**, *15*, 1805296.
[47] Z. Algharaibeh, P. G. Pickup, *Electrochem. Commun.* **2011**, *13*, 147–149.
[48] H. Fei, Y. Liu, Y. An, X. Xu, G. Zeng, Y. Tian, L. Ci, B. Xi, S. Xiong, J. Feng, *J. Power Sources* **2018**, *399*, 294–298.
[49] Y. Huang, R. Yuan, S. Zhou, *J. Mater. Chem.* **2011**, *22*, 883–888.
[50] M. Möbus, N. Karl, T. Kobayashi, *J. Cryst. Growth* **1992**, *116*, 495–504.
[51] H. Chen, Z. Zhang, Z. Wei, G. Chen, X. Yang, C. Wang, F. Du, *Sustain. Energy Fuels* **2019**, *4*, 128–131.
[52] A. A. Levin, T. Leisegang, R. Forker, M. Koch, D. C. Meyer, T. Fritz, *Cryst. Res. Technol.* **2010**, *45*, 439–448.
[53] G. Zhou, L. Mo, C. Zhou, Y. Wu, F. Lai, Y. Lv, J. Ma, Y. E. Miao, T. Liu, *Chem. Eng. J.* **2021**, *420*, 127597.
[54] W. Luo, M. Allen, V. Raju, X. Ji, *Adv. Energy Mater.* **2014**, *4*, 1400554.
[55] M. Karlsmo, R. Bouchal, P. Johansson, *Angew. Chem. Int. Ed.* **2021**, DOI 10.1002/ANIE.202111620.
[56] Q. Qu, P. Zhang, B. Wang, Y. Chen, S. Tian, Y. Wu, R. Holze, *J. Phys. Chem. C* **2009**, *113*, 14020–14027.
[57] L. Zhou, Z. Yang, C. Li, B. Chen, Y. Wang, L. Fu, Y. Zhu, X. Liu, Y. Wu, *RSC Adv.* **2016**, *6*, 109340–109345.
[58] K. Lu, B. Song, X. Gao, H. Dai, J. Zhang, H. Ma, *J. Power Sources* **2016**, *303*, 347–353.
[59] K. Krishnamoorthy, P. Pazhamalai, S. Sahoo, J. H. Lim, K. H. Choi, S. J. Kim, *ChemElectroChem* **2017**, *4*, 3302–3308.
[60] S. Zhang, Y. Liu, Q. Han, S. He, N. Zhang, J. Yang, *J. Alloys Compd.* **2017**, *729*, 850–857.
[61] S. Lindberg, N. M. Ndiaye, N. Manyala, P. Johansson, A. Matic, *Electrochim. Acta* **2020**, *345*, 136225.
[62] Q. T. Qu, B. Wang, L. C. Yang, Y. Shi, S. Tian, Y. P. Wu, *Electrochem. Commun.* **2008**, *10*, 1652–1655.
[63] "SkelCap Supercapacitor Cells," can be found under https://www.skeletontech.com/skelcap-ultracapacitor-cells?hsLang=en, **n.d.**
[64] "LG Chem E66A Batemo Cell – Get the battery model, data and report!," can be found under https://www.batemo.de/products/batemo-cell-library/e66a/, **n.d.**
[65] J. Kasnatscheew, M. Evertz, R. Kloepsch, B. Streipert, R. Wagner, I. Cekic Laskovic, M. Winter, *Energy Technol.* **2017**, *5*, 1670–1679.
[66] P. Meister, H. Jia, J. Li, R. Kloepsch, M. Winter, T. Placke, *Chem. Mater.* **2016**, *28*, 7203–7217.
[67] A. Eftekhari, *Sustain. Energy Fuels* **2017**, *1*, 2053–2060.

[68] M. Vikman, J. Vartiainen, I. Tsitko, P. Korhonen, *J. Polym. Environ.* **2015**, *23*, 206–215.
[69] C. G. VanGinkel, S. Gayton, *Environ. Toxicol. Chem.* **1996**, *15*, 270–274.
[70] K. Yapsakli, F. Çeçen, *Process Biochem.* **2010**, *45*, 355–362.
[71] "Measuring biodegradability – Science Learning Hub," can be found under https://www.sciencelearn.org.nz/resources/1543-measuring-biodegradability, **n.d**.
[72] L. Suo, O. Borodin, Y. Wang, X. Rong, W. Sun, X. Fan, S. Xu, M. A. Schroeder, A. V. Cresce, F. Wang, C. Yang, Y. S. Hu, K. Xu, C. Wang, *Adv. Energy Mater.* **2017**, *7*, 1701189.
[73] T. Jin, X. Ji, P. F. Wang, K. Zhu, J. Zhang, L. Cao, L. Chen, C. Cui, T. Deng, S. Liu, N. Piao, Y. Liu, C. Shen, K. Xie, L. Jiao, C. Wang, *Angew. Chem. Int. Ed.* **2021**, *60*, 11943–11948.
[74] L. Jiang, L. Liu, J. Yue, Q. Zhang, A. Zhou, O. Borodin, L. Suo, H. Li, L. Chen, K. Xu, Y. Hu, *Adv. Mater.* **2020**, *32*, 1904427.
[75] X. Wu, M. Sun, S. Guo, J. Qian, Y. Liu, Y. Cao, X. Ai, H. Yang, *ChemNanoMat* **2015**, *1*, 188–193.
[76] J. Chen, C. Liu, Z. Yu, J. Qu, C. Wang, L. Lai, L. Wei, Y. Chen, *Chem. Eng. J.* **2021**, *415*, 129003.
[77] X. Bu, L. Su, Q. Dou, S. Lei, X. Yan, *J. Mater. Chem. A* **2019**, *7*, 7541–7547.
[78] L. Sun, Y. Yao, Y. Zhou, L. Li, H. Zhou, M. Guo, S. Liu, C. Feng, Z. Qi, B. Gao, *ACS Sustainable Chem. Eng.* **2018**, *6*, 13494–13503.
[79] M. Song, Y. Zhou, X. Ren, J. Wan, Y. Du, G. Wu, F. Ma, *J. Colloid Interface Sci.* **2019**, *535*, 276–286.
[80] M. Pang, S. Jiang, J. Zhao, S. Zhang, R. Wang, N. Li, R. Liu, Q. Pan, W. Qu, B. Xing, *RSC Adv.* **2020**, *10*, 35545–35556.
[81] C. Karaman, O. Karaman, N. Atar, M. L. Yola, *Phys. Chem. Chem. Phys.* **2021**, *23*, 12807–12821.
[82] L. Xu, D. Yin, H. Zhao, N. Li, S. Chen, J. Xia, B. Lu, Y. Du, *Chem. A Eur. J.* **2017**, *23*, 9641–9646.
[83] T. Brousse, P. L. Taberna, O. Crosnier, R. Dugas, P. Guillemet, Y. Scudeller, Y. Zhou, F. Favier, D. Bélanger, P. Simon, *J. Power Sources* **2007**, *173*, 633–641.
[84] H. Zhang, M. Hu, Q. Lv, Z. H. Huang, F. Kang, R. Lv, *Small* **2020**, *16*, 1902843.

Manuscript received: July 2, 2022
Revised manuscript received: August 24, 2022
Accepted manuscript online: August 25, 2022
Version of record online: September 15, 2022